JOURNAL OF GEOPHYSICAL RESEARCH, VOL. 106, NO. D3, PAGES 2929–2941, FEBRUARY 16, 2001

Low-frequency temperature variations from a northern tree ring density network

Keith R. Briffa,[1] Timothy J. Osborn,[1] Fritz H. Schweingruber,[2] Ian C. Harris,[1]
Philip D. Jones,[1] Stepan G. Shiyatov,[3] and Eugene A. Vaganov[4]

Abstract. We describe new reconstructions of northern extratropical summer temperatures for nine subcontinental-scale regions and a composite series representing quasi "Northern Hemisphere" temperature change over the last 600 years. These series are based on tree ring density data that have been processed using a novel statistical technique (age band decomposition) designed to preserve greater long-timescale variability than in previous analyses. We provide time-dependent and timescale-dependent uncertainty estimates for all of the reconstructions. The new regional estimates are generally cooler in almost all precalibration periods, compared to estimates obtained using earlier processing methods, particularly during the 17th century. One exception is the reconstruction for northern Siberia, where 15th century summers are now estimated to be warmer than those observed in the 20th century. In producing a new Northern Hemisphere series we demonstrate the sensitivity of the results to the methodology used once the number of regions with data, and the reliability of each regional series, begins to decrease. We compare our new hemisphere series to other published large-regional temperature histories, most of which lie within the 1σ confidence band of our estimates over most of the last 600 years. The 20th century is clearly shown by all of the palaeoseries composites to be the warmest during this period.

1. Introduction

Many tree species display interannual growth variability that is easily measurable in terms of radial ring width or wood density changes, provided that the trees grew in areas that experience strong and regular contrasts in seasonal climates [*Fritts*, 1976; *Schweingruber*, 1988]. These tree ring data are an important source of information on past climate variability. For example, at locations where tree growth is strongly limited by growing season warmth, tree ring chronologies (i.e., annually resolved time series representing the average growth of many individual trees) may be used to reconstruct year-by-year variations in temperature, often over periods considerably longer than available local instrumental records.

Here we present reconstructed series of mean summer temperatures based on the interannual variability of wood density measured in the rings of thousands of trees growing at hundreds of sites circling the Northern Hemisphere. We use a novel data processing method when developing our chronologies to preserve potential long-term temperature changes that were not represented in early analyses of these data. We therefore provide new, independent evidence of the course of multidecadal and century-timescale summer temperature trends over large areas of the Northern Hemisphere during the last 600 years.

[1]Climatic Research Unit, University of East Anglia, Norwich, U.K.
[2]Swiss Federal Institute for Forest, Snow and Landscape Research, Birmensdorf, Switzerland.
[3]Institute of Plant and Animal Ecology, Ural Branch of the Russian Academy of Sciences, Ekaterinburg, Russia.
[4]Institute of Forest, Akagemgorodok, Krasnoyarsk, Russia.

Paper number 2000JD900617.
0148-0227/01/2000JD900617$09.00

The network of site data used here is shown in Figure 1. It has been assembled from generally cool and moist sites, near altitudinal or latitudinal tree lines, where the growth of the trees would be potentially highly sensitive to temperature forcing [*Schweingruber and Briffa*, 1996]. Each of the points in the network represents a collection of multiple tree core samples, from bark to pith, from which a number of annual or subannual growth parameters have been measured, typically over several hundred years or more. The date of ring formation is known precisely, so the measurements are associated with a rigid calendrical timescale. Such data are generally converted into time series of dimensionless indices and then averaged to form a site chronology [*Fritts*, 1976]. The most frequently used growth parameters represent either ring widths or maximum-latewood densities (MXD). The indexing is achieved by taking residuals from some low-frequency function or smoother fit to the measurements for each tree. For example, *Briffa et al.* [1998a,1998b] used residuals from a generalized exponential curve (i.e., a Hugershoff function [*Bräker*, 1981]) fit to the raw data. This indexing or "standardization" is intended to remove bias in the data series from individual trees that arises from an expected tendency for trees to lay down narrower and less dense rings as they become older. However, this approach does not distinguish between biological trends and those driven by slow changes in climate so that the resulting chronologies will not represent forcing influences on timescales that equate roughly to the length of typical tree ages or longer [*Cook et al.*, 1995; *Briffa et al.*, 1996].

The relationships between tree growth and climate (temperature and precipitation) have been previously explored in detail across the network at local and large regional scales and the MXD data used as predictors in regression-based reconstructions of regional temperatures for an optimum April-September seasonal mean [*Briffa et al.*, 1998b; K.R. Briffa et al., Tree-ring width and density chronologies around the Northern Hemisphere, 1, local and regional climate signals, submitted to *The Holocene*, 2000] (hereinafter referred to as Briffa et al. (submitted manu-

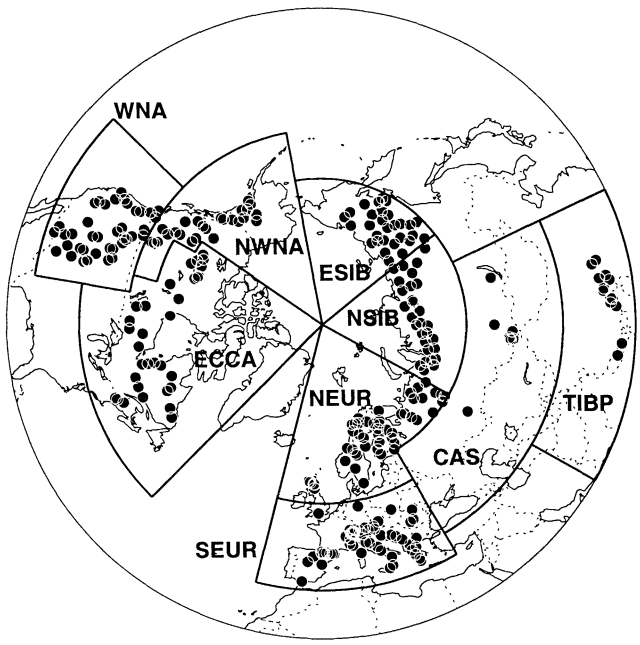

Figure 1. Locations (circles) of the 387 tree ring density chronologies, together with the boundaries of the nine arbitrary regions: NEUR, northern Europe; SEUR, southern Europe; NSIB, northern Siberia; ESIB, eastern Siberia; CAS, central Asia; TIBP, Tibetan Plateau; WNA, western North America; NWNA, northwestern North America; ECCA, eastern and central Canada.

script, 2000)). Such reconstructions represent interannual to multidecadal variations in temperature with a very high level of fidelity, but the indexing procedure used in assembling the earlier chronology predictors prohibits the representation of temperature variability on timescales of about a century and longer. So, while these reconstructions have proved valuable for studying climate variability and the role of various forcing factors acting on relatively short timescales, such as volcanic eruptions [*Briffa et al.*, 1998a], they are of limited use for judging the relative magnitude of 20th century warmth in a multicentury context. One alternative chronology construction method that can preserve long-timescale variability in tree ring data has been proposed: the regional curve standardization or RCS [*Briffa et al.*, 1996]. Ideally, however, this requires large amounts of tree growth data representing a wide range of different tree ages, each distributed widely through time and all drawn from a single species in a relatively small region [*Briffa et al.*, 1996]. It is not therefore well suited to the scale and type of analyses we are concerned with here. For this reason, we propose a different approach to capturing long-timescale, in this case temperature, variability in these data.

2. An Age Band Decomposition (ABD) Method of Chronology Construction

Figure 2 is one illustration of the expected change in MXD with increasing tree age, in this case for all scots pine (*Pinus sylvestris*) data in the network. The bold line is the average of all measured values aligned by ring age (i.e., year from pith), regardless of the calendrical date of growth. The general shape of the curve is similar for different conifer genera, growing in different regions around the hemisphere, though the precise curve parameters vary in magnitude. Typically, during the first few decades of the tree's life, density increases and levels off. After 50 years or so the trend is negative and quasilinear.

The use of this single regional mean reference curve to predict absolute density as a function of age in individual trees at different sites (equivalent to the RCS approach) would be subject to large uncertainty, as shown by the wide 1σ confidence limits about the mean curve in Figure 2. Allowing the parameters to vary so as to fit the curve to the time series of measurements from an individual tree would clearly remove low-frequency variance in the residuals, as discussed above.

The approach we explore here is to decompose the measurement data into separate subgroups defined by age class, assemble these data into individual age band time series, scale these to have equal mean and variance, and finally, recombine the scaled series for different age classes into a single series of relative growth changes. This age band decomposition (ABD) method is illustrated schematically in Plate 1. In our application, time series of MXD are made up by simple averaging of measurements derived only from rings within a specified range of tree ages, say, for example, 101 to 150 years from the pith. This is first done separately for each individual site/species collection within the geographical region of interest, though at this stage the time series may not be complete. The data available in each series are then converted into z scores (using a specified common period mean and standard deviation, in this case for 1700-1994) and averaged with all other similarly scaled site/species series for this age band. The process is repeated for each of the predetermined age bands with available data in the region. We have used a narrower banding for trees up to 100 years old (ten 10-year bands) to account for the faster rate of change in MXD with tree age in younger trees (e.g., see Figure 2) and wider bands (50 years) for older trees (see the example shown in Figure 3). The separate bands are then renormalized and averaged (using only the sections made up with data from at least two site/species collections) to produce a single regional ABD chronology. This technique was applied separately to the data from each of the nine regions shown in Figure 1 and an ABD chronology produced for each. These data were then used to estimate summer temperature variability over recent centuries in each region.

It should be noted that the interannual variability of the temperature estimates, and in particular, the relative magnitude of the individual yearly extremes do not correspond precisely with those produced by the earlier processing approach [e.g., *Briffa et al.*,

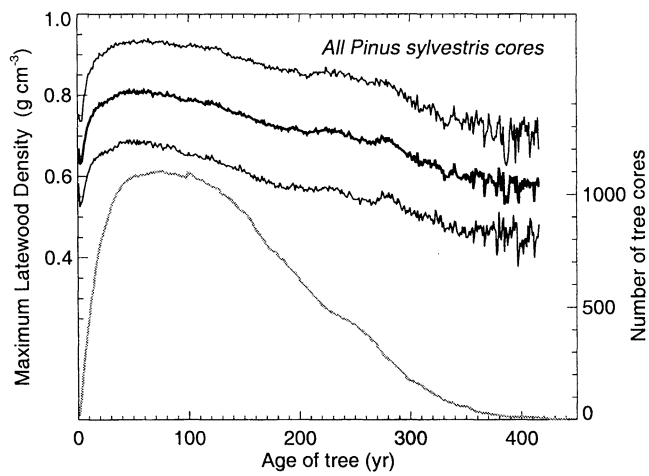

Figure 2. Maximum latewood density of each tree ring as a function of the age of the ring, for the average (thick line, with ±1 standard deviations indicated by the thin lines) over all *Pinus sylvestris* L. tree cores. Values shown for all ages that have rings from at least 10 cores (lower grey curve shows the number of tree cores with rings of each age, plotted against the right-hand scale).

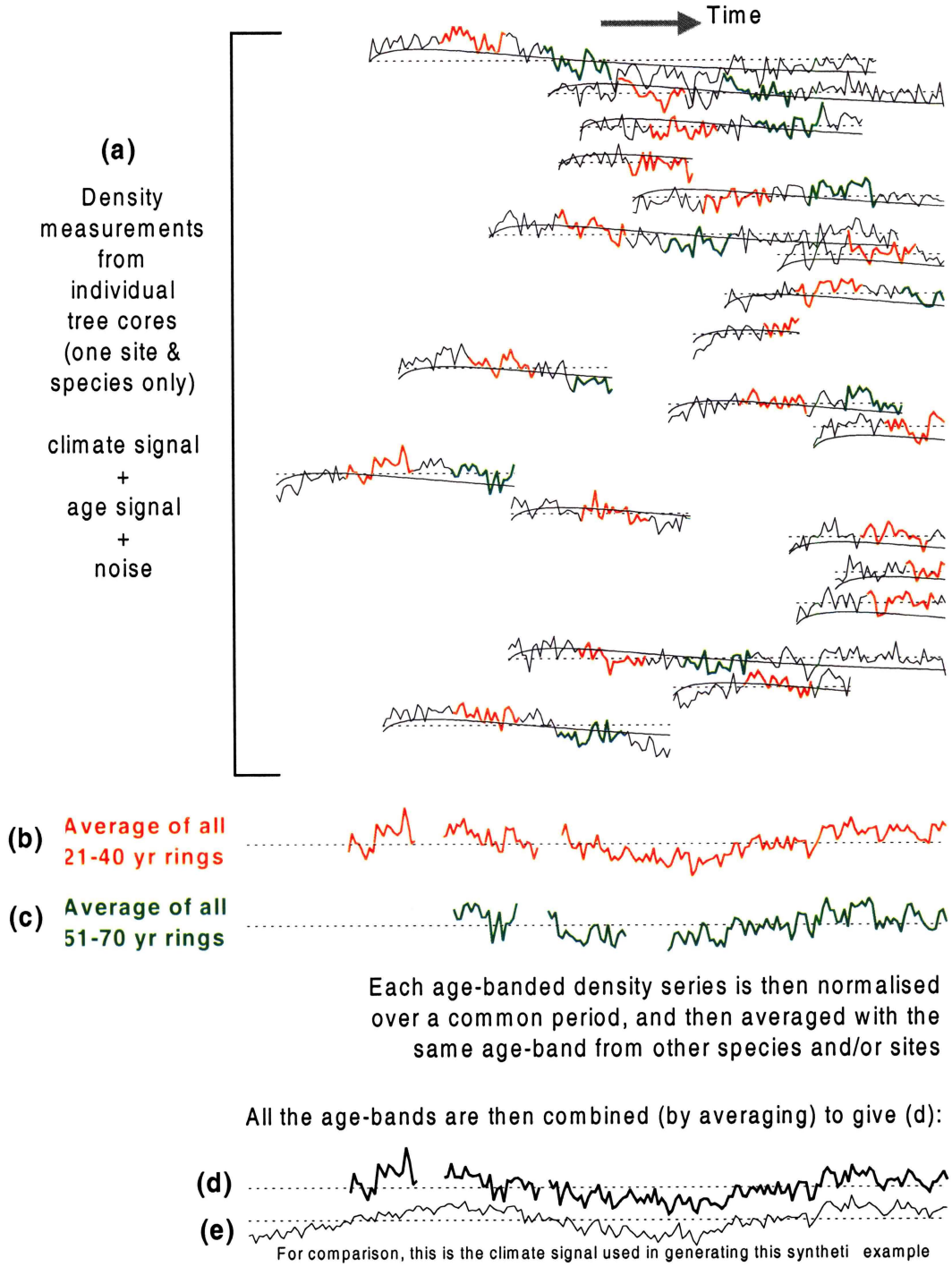

Plate 1. Schematic illustration of the age-banding procedure, using synthetic data. A synthetic climate signal (Plate 1e) is generated as a century scale sinusoid with the addition of some red noise. Twenty tree cores (Plate 1a) are generated with random starting years and lifetimes, and with a synthetic year-by-year density that is a combination of the common climate signal, red noise that differs for each core, and a function of age (with a Hugershoff-form [see *Bräker*, 1981]) that is common across all cores but that is shifted to coincide with each starting year (age functions are shown by the smoothly varying curves). The average density value for each core is shown as a horizontal dashed line. The density values from rings that are between 21 and 40 years of age are highlighted in red in (Plate 1a); these absolute values are averaged for each year to produce the 21- to 40-year age-banded series (Plate 1b). The 51- to 70-year age band is highlighted in green in (Plate 1a), with the average of the green densities shown in (Plate 1c). Each age-banded series is then normalized over a common period and averaged with the same age bands from other sites and species. Averaging all the age-banded series together (note that many more bands are used in practice, e.g., see Figure 3) produces the final time series (Plate 1d), which clearly exhibits the underlying climate forcing.

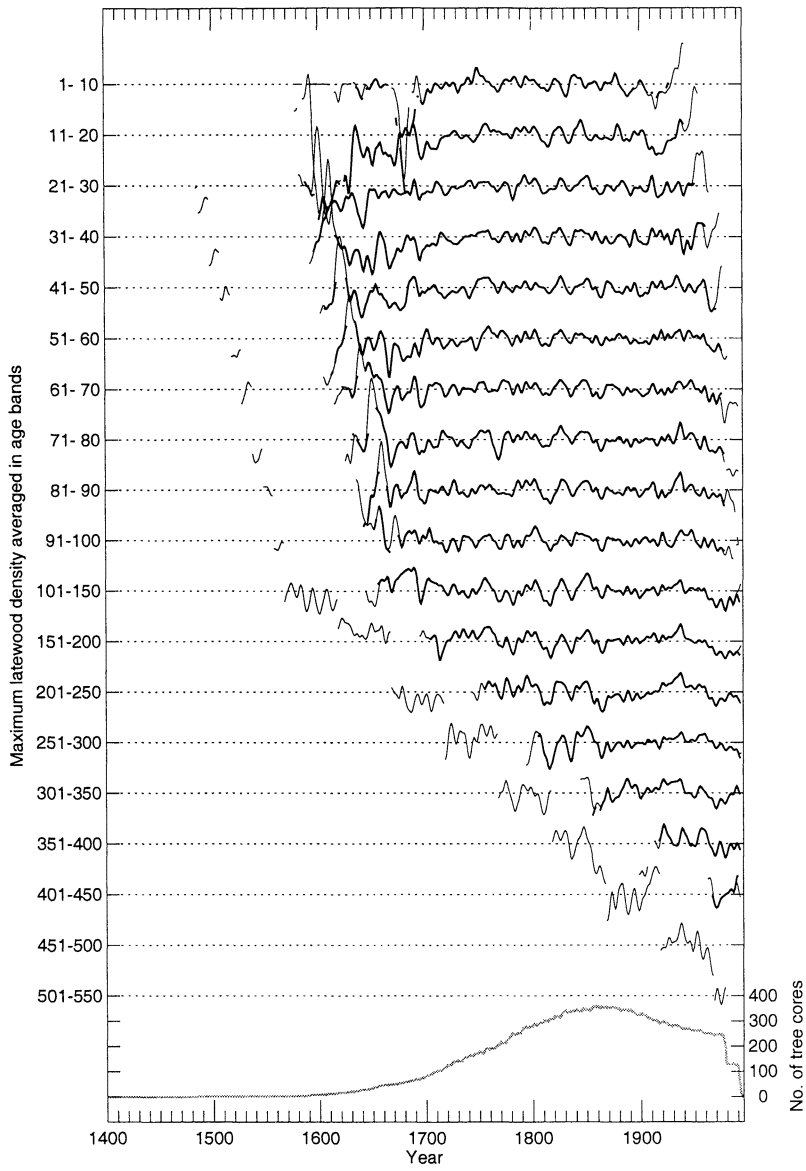

Figure 3. Age-banded time series for the northern Europe region. The curves show the average normalized tree ring density of all trees that fall into each of 19 age bands (the first 10 bands are 10 years wide, with the others 50 years wide, as indicated on the left-hand scale), smoothed with a decadal filter. Normalization was applied after all cores of one species at each site had been averaged, but before different species and sites were combined together, using the mean and standard deviation over the 1700-1994 period. The thin lines show all the data, while the thick lines show the time series when data are available from more than one site or species. The lower grey curve shows the number of tree cores with data in the region.

1998a,1998b, submitted manuscript, 2000]. In the current method, not all of the data contribute, and when they do their weighting is different from that achieved by simple, direct averaging of high-pass residual time series used in more traditional standardization techniques. We consider that high-frequency variability (interannual to decadal timescale) is therefore best expressed by the earlier processing approach, and we experiment with the current ABD method specifically in an attempt to extract greater multi-decadal, century and longer timescale variability. However, the interannual variability of the series, as processed here, still correlate very highly with the results of the earlier techniques (see Table 1).

3. Low-Frequency Regional Temperature Reconstructions

Each regional ABD MXD time series (see Figure 1) has been calibrated against an equivalent regional April-to-September mean temperature series, produced as an aggregate of the co-located grid box instrumental surface anomalies (with respect to 1961-1990 from land stations only [*Jones et al.*, 1999]). We used simple linear regression, fitting the regression equations over the period 1881-1960, or over the total available period prior to 1960 when the instrumental record was shorter (see Table 1). The period after 1960 was not used to avoid bias in the regression

Table 1. Calibration Statistics for Reconstructions of Regional and Large-Scale Temperature Series, Over the 1881-1960 Period[a]

Region	r	r, <10 years	r, >10 years	RMSE, °C	r (ABD, Hugershoff) 1881-1960	r (ABD, Hugershoff) pre-1881
NEUR	0.76	0.78	0.71	0.44	0.98	0.82
SEUR	0.65	0.62	0.71	0.37	0.95	0.91
NSIB	0.77	0.68	0.90	0.58	0.99	0.93
ESIB	0.52	0.44	0.64	0.64	0.96	0.91
CAS	0.53	0.53	0.52	0.37	0.96	0.92
TIBP	0.43	0.29	0.64	0.20	0.96	0.94
WNA	0.72	0.73	0.81	0.36	0.97	0.84
NWNA	0.65	0.72	0.62	0.46	0.95	0.85
ECCA	0.69	0.75	0.56	0.49	0.94	0.78
ALL	0.75	0.71	0.86	0.22	0.97	0.82
NH	0.68	0.53	0.84	0.19	0.98	0.85

[a]See also Figure 1. Correlations are given between the reconstruction and the temperature data for raw, high-pass and low-pass filtered data (using a 10 year filter). The root mean square error (RMSE) is the standard deviation of the residuals over the calibration period. Correlations between the high-pass filtered ABD time series and the corresponding Hugershoff-standardized series of Briffa *et al.* (submitted manuscript, 2000) are given for 1881-1960 and the pre-1881 period.

coefficients that could be generated by an anomalous decline in tree density measurements over recent decades that is not forced by temperature [*Briffa et al.*, 1998b].

The correlations are generally very high, particularly for northern Europe, northern Siberia and western North America (all greater than 0.7). The lowest are for eastern Siberia (0.52), where the optimum season is shorter than our universally applied April-to-September period (see *Briffa et al.*, submitted manuscript, 2000), central Asia (0.53), and the Tibetan Plateau (0.43), the latter two being based on considerably fewer chronologies (Figure 1) with noticeably weaker regional temperature sensitivity than was the case for the other regions (*Briffa et al.*, submitted manuscript, 2000). The Tibetan Plateau correlation at high frequency (10-year high-pass filtered data) is only 0.29, and though it is higher for the low-pass comparison (0.64), there is little long timescale variability evident in these data (see Plate 2). In terms of variance, summer temperatures in the region of the Tibetan Plateau chronologies are typically a quarter of the magnitude of those in more northerly regions of the network. Plate 2 shows all of the new, low-frequency April-September regional reconstructions, plotted here as decadally smoothed anomalies, in black. They are bracketed by their 1 and 2 standard error confidence estimates. These are time- and timescale-dependent and take into account the residual temperature variance in calibration and uncertainty (standard errors) in the regression coefficients, as well as accounting for autocorrelation in the residuals (using a method suggested by P. Bloomfield, personal communication, 1990), as described by Briffa *et al.* (submitted manuscript, 2000). An independent indication of series reliability can be calculated using the expressed population signal (EPS) [*Wigley et al.*, 1984; *Briffa and Jones*, 1990] which measures the expression of common variability among the available age band time series through time. The EPS has been calculated here using the number of bands with data and the strength of their correlation with each other, and the vertical red lines in Plate 2 indicate where this measure of EPS for each series falls below an arbitrary value of 0.5.

Comparison of the new temperature estimates with those derived from chronologies produced using earlier approaches to standardization (in blue) shows the new estimates to be generally colder in almost all periods. The most significant difference is seen during the first half of the 17th century, in northern Siberia [see *Naurzbaev and Vaganov*, 2000]. However, similar evidence of accentuated coolness at this time is seen in northern Europe, and in southern Europe and western North America, where the whole century is now cooler. One very notable exception to the generally lower temperatures in our new estimates is clearly apparent for the whole of the 15th century in northern Siberia, where the new reconstruction is significantly warmer, perhaps more so, on average, than the observed mean for the 20th century (though the early data have wide uncertainty estimates that easily overlap 20th century temperatures).

4. Northern Hemisphere "Extratropical" Land Temperature Series

Given the widespread coverage of the tree ring density chronologies (Figure 1), it is possible to produce a reconstruction of a single growing season temperature series representing a large fraction of the Northern Hemisphere. No attempt is made here to reconstruct the mean temperature of the entire hemisphere, due to the obvious constraints of the chronology locations (land only and extra tropical). Instead, reconstructions of two, highly correlated ($r = 0.89$ over 1860-1994), observed area averages are produced, both for the April-to-September season: the average of all air temperatures over land north of 20°N (NH) and the average of all air temperatures in land grid boxes that also have at least one tree chronology in them (ALL). However, our chosen temperature predictands are highly correlated with "full" Northern Hemisphere annual temperatures (e.g., over 1881-1960, NH is correlated at 0.81, or 0.92 for decadally smoothed data and 0.53 for 10-year high-pass filtered data).

A variety of methods can be used to transform the multitude of density chronologies into a single calibrated large-scale temperature series. The site chronologies can be combined using an unweighted or weighted sum (or average) of all the data. Alternatively, appropriate weighting might be applied solely on the basis of the characteristics (e.g., reliability) of the individual series, or in order to provide a best fit to the target series (e.g., multiple linear regression). Previous work aimed at aggregating various proxy records to estimate Northern Hemisphere mean temperatures have used scaled simple unweighted averages [e.g., *Jones et al.*, 1998; *Crowley and Lowery*, 2000], weighting based

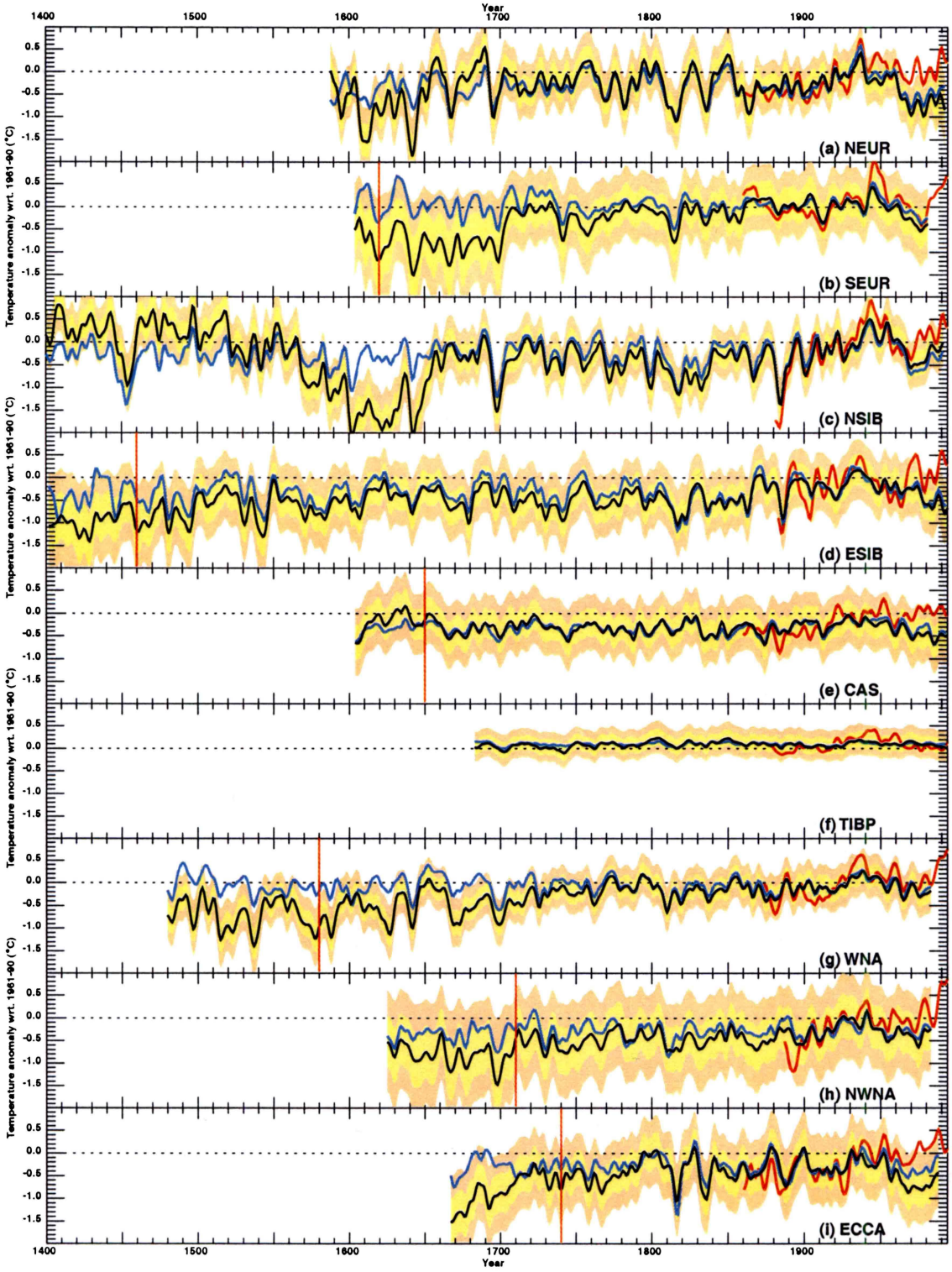

Plate 2. Reconstructions of nine regional April-September temperature series, all with decadal smoothing. Observed temperatures are shown in red, Hugershoff-standardized reconstructions are shown in dark blue, age-banded reconstructions are shown in black (with ±1 and ±2 standard errors indicated by the yellow and orange shading). The vertical red lines in some reconstructions indicate how far back the age-banded reconstructions are considered to be reliable (see text for further details).

on internal estimates of proxy series reliability (*Briffa et al.*, submitted manuscript, 2000), and multiple regression [e.g., *Mann et al.*, 1998]. Bias might be introduced in cases where the spatial coverage is non uniform (e.g., of the 24 original chronologies with data back to 1500, half are concentrated in eastern Siberia), but this can be reduced by prior averaging of the chronologies into regional series (as was done in the previous section). Subsequently, calibration of the single series obtained can be achieved either by regression against the observed series, or by scaling the reconstruction so that it has the same mean and variance as the observed record over some common period. In the present study we use only regression (which, by definition, minimizes the variance of the residuals), but note that the scaling approach (as used by *Jones et al.* [1998], for example) also has its merits.

Eight different methods have been used here to generate a reconstruction of the ALL temperature record (Figure 4; further details in Appendix A). They produce very similar results for the post-1700 period and can barely be distinguished on the basis of their correlation with the instrumental series (all methods produce correlations with the observed temperatures that are between 0.71 and 0.79). They exhibit fairly dramatic differences, however, in the magnitude of multidecadal variability prior to 1700, though the timing of this variability remains well correlated. The difference in reconstruction spread before and after 1700 is remarkable, highlighting the sensitivity of the reconstruction to the methodology used, once the number of regions with data, and the reliability of each regional reconstruction, begin to decrease. The selection of a single reconstruction of the ALL temperature series is clearly somewhat arbitrary.

The eight methods also produce a similar spread prior to 1700 when applied to the reconstruction of the NH time series (of land temperatures north of 20°N), yet are also similar post-1700 and also exhibit a narrow range of correlations against the instrumental series (in the range $r = 0.64$ to 0.69). The method that produces the best fit in the calibration period is principal components regression (PCR, the thick curve in Figure 4); this might be expected, given the additional parameters that are available in this method for obtaining a good fit to the observations, but the reconstruction passes a careful, independent verification (see Appendix A). The PCR-based curve is selected therefore as the preferred reconstruction for both the NH and ALL temperature averages. The calibration statistics of these reconstructions are included in Table A1.

Figure 5 shows the large-scale temperature estimates that make up the ALL series, again illustrating the time-dependent and timescale-dependent nature of their associated uncertainties, the former being a consequence of the diminution in available data in the earlier period. The very close correspondence with the target temperature data on the interannual timescale is evident (top panel), as is the gradual divergence in trends during recent decades mentioned earlier, and discussed by *Briffa et al.* [1998b, submitted manuscript, 2000]. The clear evidence of this in these (differently processed) data demonstrates that the phenomenon is not a product of the standardization technique used in the earlier studies. Despite some small differences in the interannual variability between the earlier and newly processed data, also mentioned above (e.g., the relative coldness of 1601 and 1453 is not ranked as extreme as previously), the same strong interdecadal variability in the new temperature estimates reemphasizes the relative cold of the 1640s, 1660s, and 1770s, the decade centered on 1700, and the 1810s and 1830s. However, there is now new evidence that the high variability of the 17th century is superimposed on a strong temperature depression that extends throughout the late 16th century, all of the 17th century, and into the early 18th centuries.

The regional expression of this cool phase is clear in the western North America series (compare Plate 2) and in the earlier (and less reliable) sections of the series for northern and southern Europe, northwest North America, and eastern Canada. In the northern Siberian data, it is the late 16th and first half of the 17th centuries that are very cool. However, this widespread and protracted period of cold summers is not evident in the data from eastern Siberia.

In Figure 6, we combine the evidence for long-timescale summer temperature change around the northern extratropics with the evidence of high-frequency variability derived from earlier work [e.g., *Briffa et al.*, 1998a,1998b] to provide what we consider to be the most reliable indication of large-scale summer (April-September) temperature across a range of timescales that can be extracted from our current densitometric tree-ring data for the last six centuries. Power spectrum analysis of these series (Figure 7) reveals the same short-term concentrations of variance at periods near 2.4, 3.7, 5.3, and 6.7 years that were evident in the

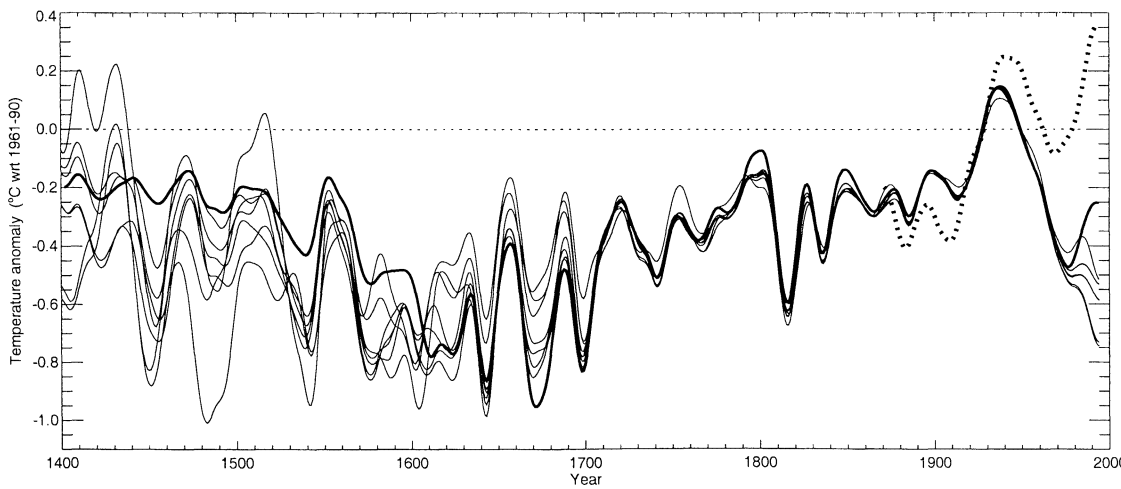

Figure 4. Eight alternative reconstructions of the mean temperature over all land north of 20°N (observations shown by dotted line for 1871-1994). All curves are smoothed with a 25-year filter. See text for explanation of the eight reconstruction methods. The preferred reconstruction based on principal components regression is shown by the thick line for 1402-1994.

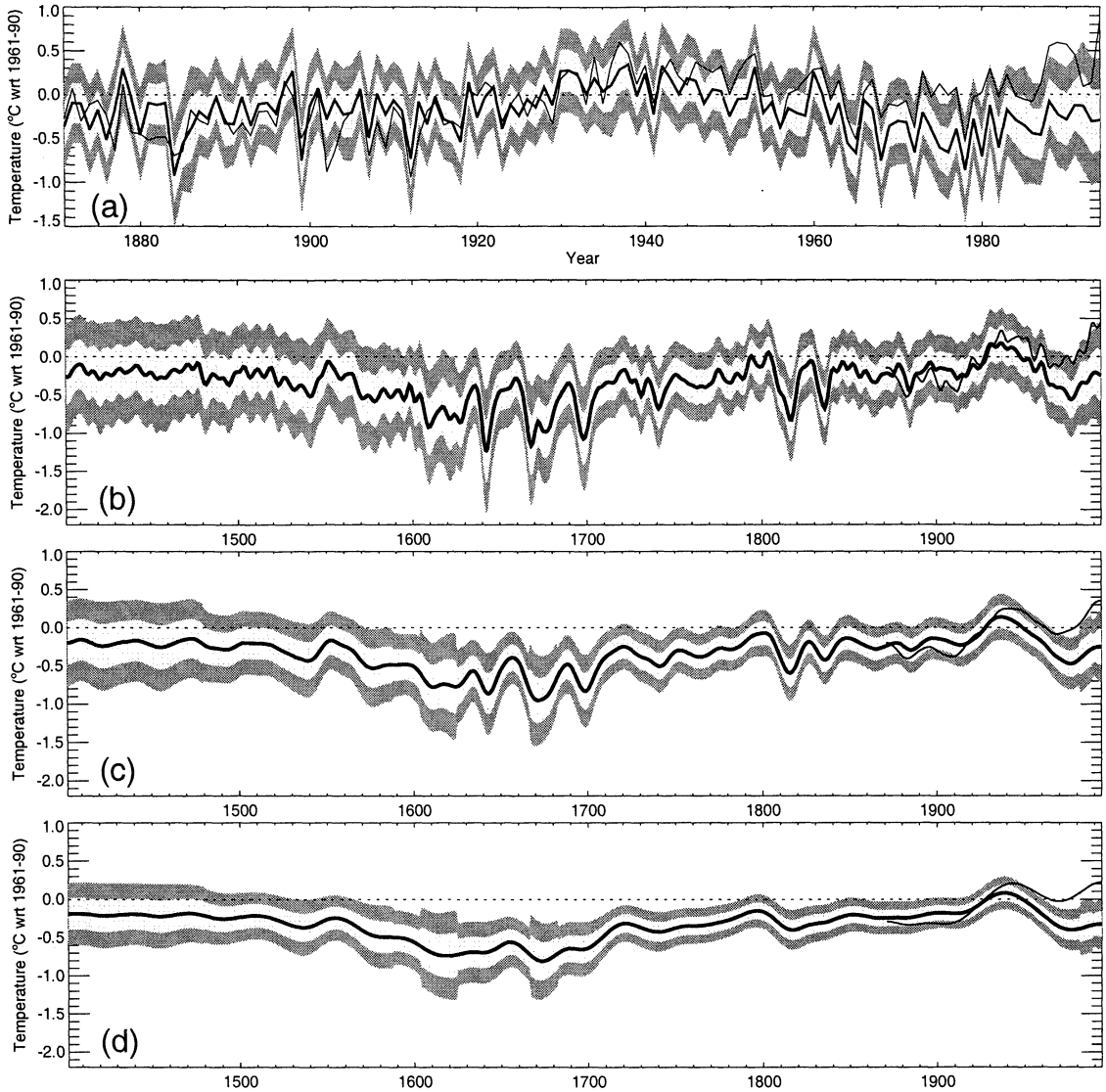

Figure 5. Principal components regression reconstruction (thick line) of the ALL temperature series (thin line), with shading to indicate the ±1 and ±2 standard errors around the reconstruction. (a) Unfiltered data for the period with instrumental data; data smoothed by (b) 10-year, (c) 25-year, and (d) 50-year filters.

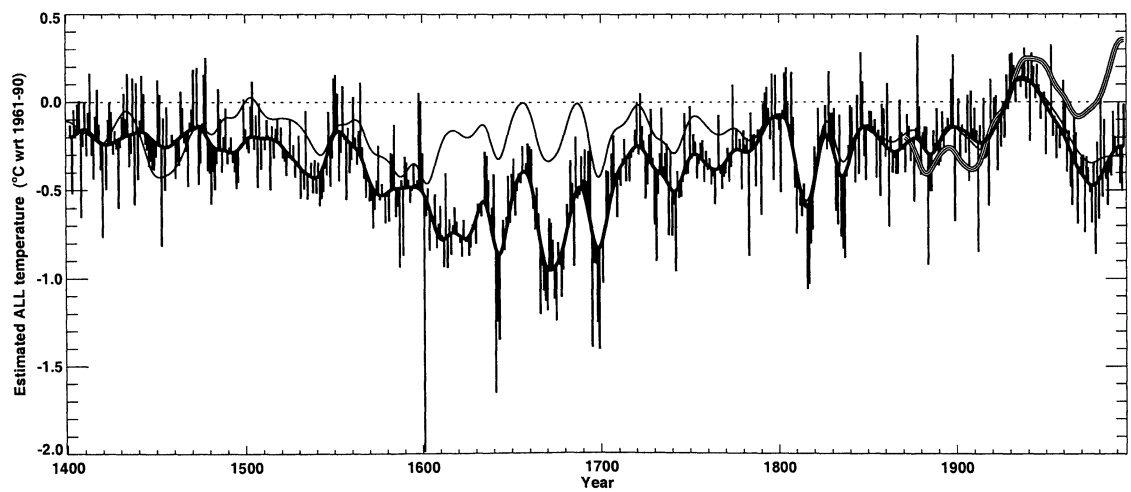

Figure 6. The 25-year smoothed age-banded reconstruction of the ALL temperature series, combined with the 25-year high-pass filtered variability from the "Hugershoff standardized" reconstruction [*Briffa et al.*, 1998a], the latter shown as annual bars above and below the 25-year variations. The thin smooth curve shows the 25-year smoothed Hugershoff standardized reconstruction. The striped curve shows the 25-year smoothed observed record.

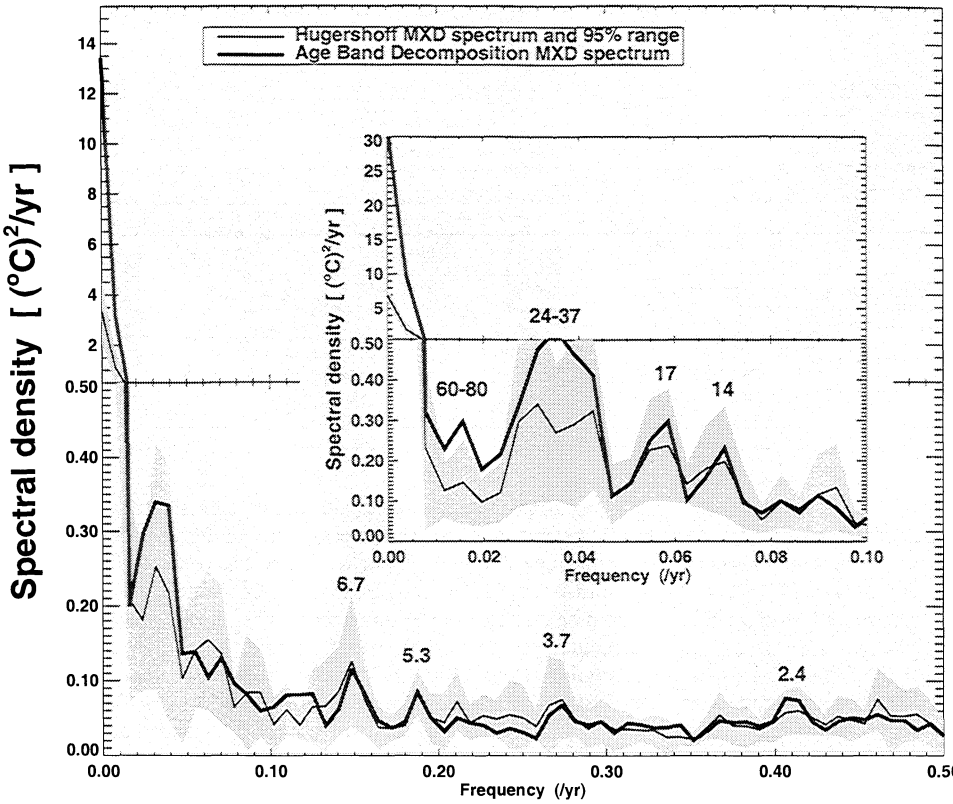

Figure 7. Comparison of spectral density of the ALL reconstructions based on tree ring density chronologies with Hugershoff standardization to remove the age effect (thin line) and that based on the new ABD technique (thick line). The spectra were estimated using the method of *Welch* [1967], dividing each series into nine overlapping segments of 128 years, windowed using a Hanning window. The 95% confidence range, based on the nine spectral estimates, is shown in grey around the Hugershoff series. Note the change in linear scale at 0.5 $(°C)^2$ yr^{-1}. The inset shows the decadal and longer timescales using higher-resolution spectra. Some dominant periodicities (years) are marked on the figure.

earlier processing of these data, but a distinct concentration of variance at about 24-37 years is now strongly accentuated, and a resolvable concentration of variance centered around 60-80 years is also now apparent. The detailed time-dependent spectral characteristics of these data will be discussed elsewhere.

5. Comparison of the New Temperature Record With Published Series

An accurate and quantitative history of mean surface temperatures across the globe is one fundamental requirement for establishing the significance of different natural forcings in the past and for identifying the scale of anthropogenic forcings during the 20th century and beyond. This need has stimulated a number of recent attempts to combine the evidence of various palaeoclimate records, either direct or indirect temperature proxies, to provide reconstructions of average Northern Hemisphere temperatures for a number of centuries prior to the availability of widespread instrumental records. Many "hemisphere" reconstructions are not independent because a general scarcity of long, high-resolution palaeorecords has led to a strong element of overlap in the data used in the different studies [*Briffa and Osborn*, 1999]. Some of these incorporate a wide geographic spread within the input data [*Bradley and Jones*, 1993; *Jones et al.*, 1998; *Mann et al.*, 1999], while others use records from a more restricted (northern), regional context [*Overpeck et al.*, 1997; *Jacoby and D'Arrigo*, 1989; *Briffa*, 2000]. Several of the hemisphere reconstructions were originally scaled by comparison with temperatures, either annual [*Mann et al.*, 1998, 1999; *Crowley and Lowery*, 2000] or summer [*Jones et al.*, 1998; *Briffa*, 2000], and with the notable exception of the Mann *et al.* work, they generally do not explicitly represent uncertainty associated with these extended reconstructions (note also that the Overpeck *et al.* series was not calibrated at all).

In Plate 3 we reproduce a number of these reconstructed series, all 50-year smoothed, superimposed on the new reconstruction described here, and its 1 and 2 standard error confidence bands. Note that our densitometric database is virtually independent of the predictors used in the other reconstructions.

We have chosen to rescale all of the records by linear regression against the same northern land area summer temperature series used to calibrate our reconstruction. Calibration of all reconstructions against the same target series and over the same calibration period (1881-1960) reduces the potential differences due to calibration issues, though we acknowledge that the selected region and season may not be optimal for all reconstructions. The only exception is that the 1901-1919 period is omitted when calibrating the *Crowley and Lowery* [2000] series, because of a poor fit during this period. We do not advocate such an approach but simply follow the procedure used by Crowley and Lowery themselves (in fact they omit the longer 1881-1919 period when calibrating against annual mean temperature).

The immediate conclusion from this comparison is that our new record is more similar to all of the other records in terms of low-frequency variability than was implied by previous comparisons [e.g., *Jones et al.*, 1999] that used our earlier series, which had not been processed using the ABD method to maintain long-

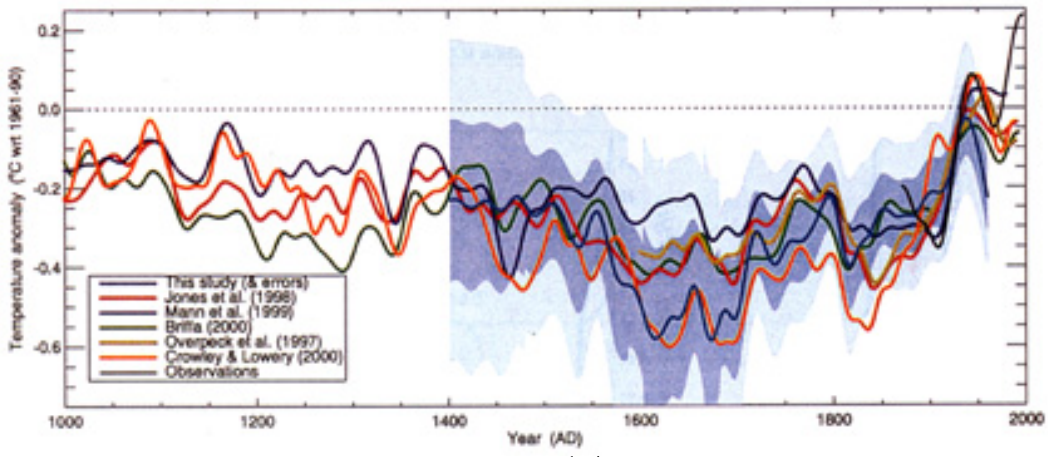

Plate 3. Comparison of six large-scale reconstructions, all recalibrated with linear regression against the 1881-1960 mean April-September observed temperature averaged over land areas north of 20°N. All series have been smoothed with a 50-year Gaussian-weighted filter and are anomalies from the 1961-1990 mean. Observed temperature for 1871-1997 (black) from *Jones et al.* [1999]; circum-Arctic temperature proxies for 1600-1990 (yellow) from *Overpeck et al.* [1997]; northern hemisphere temperature proxies for 1000-1980 (red) from *Jones et al.* [1998]; global temperature and non-temperature proxies for 1000-1980 (purple) from *Mann et al.* [1998, 1999]; three northern Eurasian tree ring width chronologies for 1000-1993 (green) from *Briffa and Osborn* [1999]; 13 Northern Hemisphere temperature proxies for 1000-1987 (orange) from *Crowley and Lowery* [2000], but excluding the two low-resolution records used by them; and the NH reconstruction from the age-banded analysis presented in this study for 1402-1960 (blue), bounded by ±1 and ±2 standard errors.

timescale variability. There is actually a high degree of correspondence between all of the curves for almost the whole of the last 600 years (correlations given in Table 2), with most of the series lying within the 1 standard error confidence band. The minor exceptions occur around the 1950s and 1960s, where three curves imply cooler conditions and throughout the 17th century when the *Mann et al.* [1998] curve indicates a less cool hemispheric excursion. This could be because the Mann *et al.* study easily had the largest geographical range of constituent data, with many predictors coming from outside the (northern) area of our tree ring data. Also, many of the tree ring series used by *Mann et al.* [1998] (e.g., northern Siberia, where we reconstruct a strong cool phase) were processed using methods not likely to preserve as much of the long timescale variability as captured by our ABD approach. However, all of the curves generally lie within the 2 standard error band for the last 600 years. Our curve and the Crowley and Lowery curve suggest that the coolest conditions were maintained for the whole of 17th century. All curves show strong warming through the early 1700s, relatively stable temperatures for the remainder of the 18th century, abrupt cooling in the early 19th century, and the expected rapid warming at the turn of the 20th century. The 20th century is clearly shown by all of the palaeoseries to be the warmest in the last 600 (and the last 1000) years. Strong, decadal-scale similarities between reconstructions are also apparent: the warm interval that interrupted the general coolness of the 1600s, the relatively warm 1560s, the cold 1810s and 1450s. The last of these is not marked in our final reconstruction, but we note that the 1450s were much cooler in all of the other (i.e., not PCA regression) methods of producing this curve (compare Figure 4). In the period before the start of our record, sharp, cool excursions are also clear in the early 1100s and at around 1200 and 1340. The few warm decades at periods near the ends of both the 11th and 12th centuries are also widely registered but are still reconstructed at about 0.1°C below the 1961-1990 mean (50-year smoothed data) [see also *Crowley and Lowery*, 2000].

Table 2. Cross correlations Between NH Temperature Reconstructions Over the Common Overlap Period 1402-1960 (1750-1960 for *Overpeck et al.* [1997])[a]

	Reference	1	2	3	4	5	6
1	This study	-	0.76	0.43[b]	0.86	0.74	0.81
2	*Jones et al.* [1998]	0.62	-	0.71	0.78	0.95	0.81
3	*Mann et al.* [1998, 1999]	0.36	0.46	-	0.60	0.86	0.64
4	*Briffa* [2000]	0.56	0.48	0.40	-	0.84	0.84
5	*Overpeck et al.* [1997]	-	-	-	-	-	0.87
6	*Crowley and Lowery* [2000]	-	-	-	-	-	-

[a]Correlations between unfiltered series (i.e., yearly values when they exist) below the diagonal and between 50-year smoothed series above the diagonal.

[b]The correlation with the average of the *Mann et al.* [1998] grid box reconstructions over the same region represented by our series is slightly higher at 0.51.

6. Conclusions

The age band decomposition (ABD) approach to tree ring chronology construction appears to be a useful addition to the range of processing methods employed to remove sample age-related bias in radial tree growth measurements such as ring width and latewood ring density. Where the raw data contain a reasonable temporal distribution of different tree age samples, this approach has the potential to express more low-frequency variability in the final chronology than many other approaches. However, we consider that interannual variability is better expressed using already available techniques. We have used the ABD approach to provide new reconstructions of summer temperatures over nine large, extratropical regions of the Northern Hemisphere, and we present a new reconstruction of low-frequency, quasi Northern Hemisphere, summer temperatures for the last 600 years. There are strong similarities in the major features of this curve and a number of other virtually independent published reconstructions of past annual or summer temperature trends: very cool conditions throughout the 17th century, strong warming in the early 1700s; abrupt cooling in the early 19th century, and clear evidence of rapid 20th-century warming to levels of warmth that are apparently unprecedented in the last 600, and probably 1000, years.

Further experimentation is required to explore the appropriateness of the ABD technique across a range of ecological situations (e.g., drought-stressed sites, higher density of trees, etc.) and different geographic scales, and to test the sensitivity of the results to the details of its implementation (i.e., using different age-band widths, different normalization options). This experimentation should also include detailed comparisons with the regional curve standardisation (RCS) approach [*Briffa et al.*, 1996] which, though having the potential to express long-timescale climate variability in tree ring data, was considered inappropriate for the scale of analysis described here.

Appendix A: Constructing Pseudo "Hemispheric" Temperature Series

In Figure 4 we show different temperature reconstructions of the NH (all land area temperatures north of 20°N), each based on a different way of using the MXD predictor data. One curve was produced by performing the age-banding procedure on all chronologies in the data set and by using an unweighted mean of all banded series from all locations. This is similar to the curve from 1650-1960 presented by *Briffa and Osborn* [1999] (although we have since made very minor modifications to the age-banding procedure and the input data set). All other curves in Figure 4 were obtained by prior averaging of the age-banded density series into the nine subregions (as defined in Figure 1). The regional series are averaged with uniform weighting in three of the curves, while for others the weighting is based upon a measure of the time-dependent reliability of each regional series (i.e., the expressed population signal (EPS) [*Wigley et al.*, 1984; *Briffa and Jones*, 1990]) computed from the number of age-bands averaged and the average correlation between them.

The preferred curve (bold in Figure 4) is produced from a multiple linear regression against the observed series, where the predictors are the principal components of the nine regional tree ring density series (i.e., principal components regression, see below). Two of the curves use only density from rings that are between 51 and 300 years of age, whilst two others use all rings that are from 21 to 550 years of age (although the additional young and old rings are not given a high weighting). Two curves use all age-banded series that fall within the appropriate age range (51 to 300 years), while all other curves omitted those parts of the age bands that had data from only one site within the region (cases that are more likely to be biased by nonclimatic signals, as shown in Figure 3). At all stages where the averaging of different age-banded time series or the averaging of different regional time series is done, and the number of time series changes through time, the variance of the average is adjusted to remove artificial changes related to the changing number of constituent time series [*Osborn et al.*, 1997].

Three of the curves in Figure 4 are based therefore on the regional series (prior to their calibration) shown in Plate 2 and discussed in section 3. The only differences are in how the regions are weighted when summed/averaged together (one has no weighting, one has reliability weighting, and one has multiple regression coefficients).

The large-area temperature averages (ALL, which is the air temperature averaged over all land grid boxes that contain a tree ring chronology, and NH, which is the air temperature averaged over all land north of 20°N) are reconstructed using the preferred method of principal components regression (PCR). The potential predictors are the leading six principal components of the nine regional-mean density chronologies (which are shown, after calibration, in Plate 2). These are input to a stepwise screening regression, which selects those predictors whose partial correlations are significant with 95% confidence during the 1906-1960 calibration period (once again, the post-1960 period is not used for calibration or verification, due to the non-temperature-related decline in tree ring density over recent decades). The regression is then verified against temperatures from the independent period 1871-1905. If the verification indicates adequate skill, then the regression is recalibrated (using the same selected principal components as predictors) over the same 1881-1960 period used in all other reconstructions reported in this paper.

The principal component analysis of the regional density series requires complete data. This necessitates building a number of different PCR models, each based on the principal components of a subset of the nine regions that have data for a particular period. For example, from 1604 to 1624, only six of the regions have data (see Table A1). The reconstruction for this period is therefore built using the six principal components of these six regional time series. For those periods with less than six regions with data, there are less than six principal components and therefore less than six potential predictors.

The potential predictors, along with the calibration and verification statistics for the model used for each period, are shown in Table A1 for both the ALL and the NH reconstructions. The multiple regressions are all statistically significant with 99% confidence when calibrated. The verification skill is measured by the correlation and by the reduction of error (*RE*) statistics [*Fritts et al.*, 1990; *Cook et al.*, 1994]. The verification correlations decrease slightly for the models built using the principal components of fewer regions, although they are statistically significant with the exception of the periods 1402-1479 and 1992-1994. Verification of the decadal timescale variability results in notably higher correlations, even for the early models that use fewer regions. The *RE* statistic also measures the skill at reproducing the lower mean during the verification period; a common assumption is that any $RE > 0$ is considered to represent significant regression skill. All PCR models easily pass this threshold. As all models are considered to have useful skill, all are recalibrated over the 1881-1960 period, with calibration correlations also indicated in Table A1. The models based on fewer regional series show a decrease in skill, but this is mainly at the higher frequencies. Fewer principal components (typically only the leading one) pass the screening regression for the NH series than for the ALL series. This results in somewhat higher variance captured during calibration of ALL, and the verification statistics are also better.

Table A1. Calibration and Verification Statistics for the Principal Components Regression Reconstructions of the ALL and NH Temperature Series[a]

	Predictors:	Calibration (1906-1960)	Verification (1871-1905)		Final calibration (1881-1960)		
Period	(*N*) PC number	*r*	*r*	*RE*	*r*	*r*, <10 years	*r*, >10 years
				ALL			
1402-1479	(2) 1	0.33	0.19	0.28	0.40	0.09	0.70
1480-1587	(3) 1	0.49	0.34	0.42	0.53	0.31	0.78
1588-1603	(4) 1 4	0.66	0.53	0.58	0.67	0.63	0.81
1604-1624	(6) 1 2 3 6	0.73	0.52	0.49	0.71	0.67	0.86
1625-1666	(7) 1 2	0.67	0.41	0.51	0.68	0.55	0.85
1667-1682	(8) 1 2 5	0.77	0.50	0.36	0.75	0.73	0.84
(1683-1981	(9) 1 2 5	0.79	0.54	0.40	0.75	0.71	0.86)
1982-1988	(6) 1 2	0.66	0.49	0.42	0.65	0.61	0.78
1989-1991	(5) 1 2	0.60	0.45	0.47	0.61	0.46	0.81
1992-1994	(3) 1 3	0.45	0.24	0.10	0.39	0.17	0.74
				NH			
1402-1479	(2) 1	0.37	0.33	0.30	0.42	0.10	0.69
1480-1587	(3) 1	0.46	0.33	0.33	0.49	0.20	0.76
1588-1603	(4) 1	0.56	0.42	0.39	0.59	0.41	0.78
1604-1624	(6) 1 2	0.59	0.43	0.39	0.61	0.44	0.81
1625-1666	(7) 1	0.57	0.27	0.26	0.57	0.33	0.80
1667-1682	(8) 1	0.65	0.41	0.37	0.65	0.51	0.81
(1683-1981	(9) 1	0.68	0.44	0.38	0.68	0.53	0.84)
1982-1988	(6) 1	0.62	0.56	0.50	0.66	0.57	0.79
1989-1991	(5) 1	0.57	0.47	0.43	0.60	0.41	0.79
1992-1994	(3) 1 3	0.44	0.28	0.11	0.43	0.18	0.77

[a]The period over which each model is used, the number of regions (*N*) with data for that period, and the principal components that are selected as predictors are listed. The main model is shown in parentheses. Due to the successful verification of all models, they are all recalibrated over the 1881-1960 period, and correlations are given for this period between the reconstruction and the temperature data for raw, high-pass and low-pass filtered data (based on a 10-year filter).

Finally, note that the regressions were built and tested using the full data set (although subsets of the regional time series were used for each of the different models, according to the period during which the model was to be used; see Table A1). To compute the uncertainty bands shown in Figure 5 and Plate 3, however, an additional time-dependent deterioration in skill is taken into account: the number of chronologies with data decreases, even if a particular region still has data. A fixed-grid approach is used: regional time series are constructed using only those chronologies that have data back to the required time (*t*), and these are put through the principal components regression model applicable at time *t* and compared with the instrumental record. The residual variance and the uncertainties in the regression model parameters are used to quantify the uncertainty range at time *t*, as described by Briffa *et al.* (submitted manuscript, 2000).

Acknowledgments. This work was funded by U.K. NERC (GR3/12107) and the EC under ADVANCE-10K (ENV4-CT95-0127). P.D.J. acknowledges support of the U.S. Department of Energy (DE-FG02-98ER 62601). We thank Ä. Brauning for allowing us to use the Tibetan Plateau data.

References

Bradley, R.S., and P.D. Jones, 'Little Ice Age' summer temperature variations: their nature and relevance to recent global warming trends, *Holocene*, *3*, 367-376, 1993.

Bräker, O., Der Alterstrend bei Jarringdichten und Jahrringbreiten von Nadelhölzern und sein Ausgleich, *Mitt. Forstl. Bundesvers Anst Wien*, *142*, 75-102, 1981.

Briffa, K.R., Annual variability in the Holocene: interpreting the message of ancient trees, *Quat. Sci. Rev. 19*, 87-105, 2000.

Briffa, K.R., and P.D. Jones, Basic chronology statistics and assessment, in *Methods of Dendrochronology: Applications in the Environmental Sciences*, edited by E.R. Cook and L.A. Kairiukstis, pp. 137-152, Kluwer Acad., Norwell, Mass., 1990.

Briffa, K.R., and T.J. Osborn, Seeing the wood from the trees, *Science*, *284*, 926-927, 1999.

Briffa, K.R., P.D. Jones, F.H. Schweingruber, W. Karlén, and S.G. Shiyatov, Tree-ring variables as proxy-climate indicators: Problems with low-frequency signals, in *Climate Variations and Forcing Mechanisms of the Last 2000 Years*, edited by P.D. Jones, R.S. Bradley, and J. Jouzel, pp. 9-41, Springer-Verlag, New York, 1996.

Briffa, K.R., P.D. Jones, F.H. Schweingruber, and T.J. Osborn, Influence of volcanic eruptions on Northern Hemisphere summer temperature over the last 600 years, *Nature*, *393*, 450-455, 1998a.

Briffa, K.R., F.H. Schweingruber, P.D. Jones, T.J. Osborn, S.G. Shiyatov, and E.A. Vaganov, Reduced sensitivity of recent northern tree-growth to temperature at northern high latitudes, *Nature*, *391*, 678-682, 1998b.

Cook, E.R., K.R. Briffa, and P.D. Jones, Spatial regression methods in dendroclimatology: A review and comparison of two techniques, *Int. J. Climatol.*, *14*, 379-402, 1994.

Cook, E.R., K.R. Briffa, D.M. Meko, D.A. Graybill, and G. Funkhouser, The 'Segment Length Curse' in long tree-ring chronology development for palaeoclimatic studies, *Holocene*, *5*, 229-237, 1995.

Crowley, T.J., and T.S. Lowery, How warm was the Medieval Warm Period?, *Ambio*, *29*, 51-54, 2000.

Fritts, H.C., *Tree Rings and Climate*, 567 pp., Academic, San Diego, Calif., 1976.

Fritts, H.C., J. Guiot, and G.A. Gordon, Verification, in *Methods of Dendrochronology*, edited by E.R. Cook and L.A. Kairiukstis, pp. 178-185, Kluwer Acad., Norwell, Mass., 1990.

Jacoby, G.C., Jr., and R.D. D'Arrigo, Reconstructed Northern Hemisphere annual temperatures since 1671 based on high-latitude tree-ring data from North America, *Clim. Change*, *14*, 39-59, 1989.

Jones, P.D., K.R. Briffa, T.P. Barnett, and S.F.B. Tett, High-resolution palaeoclimatic records for the last millennium: Interpretation, integration and comparison with control-run temperatures, *Holocene*, *8*, 455-471, 1998.

Jones, P.D., M. New, D.E. Parker, S. Martin, and I.G. Rigor, Surface air temperatures and its changes over the past 150 years, *Rev. Geophys.*, *37*, 173-199, 1999.

Mann, M.E., R.S. Bradley, and M.K. Hughes, Global-scale temperature patterns and climate forcing over the past six centuries, *Nature*, *392*, 779-787, 1998.

Mann, M.E., R.S. Bradley, and M.K. Hughes, Northern Hemisphere temperatures during the last millennium: Inferences, uncertainties and limitations, *Geophys. Res. Lett.*, *26*, 759-762, 1999.

Naurzbaev, M.M., and E.A. Vaganov, Variations of early summer and annual temperature in the east Taymir and Putoran over the last two millennia inferred from tree rings, *J. Geophys. Res.*, *105*, 7317-7327, 2000.

Osborn, T.J., K.R. Briffa, and P.D. Jones, Adjusting variance for sample-size in tree-ring chronologies and other regional mean timeseries, *Dendrochronologia*, *15*, 89-99, 1997.

Overpeck, J., et al., Arctic environmental change of the last four centuries, *Science*, *278*, 1251-1256, 1997.

Schweingruber, F.H., *Tree Rings. Basics and Applications of Dendrochronology*, 276 pp., Kluwer Acad., Norwell, Mass., 1988.

Schweingruber, F.H., and K.R. Briffa, Tree-ring density networks for climate reconstruction, in *Climate Variations and Forcing Mechanisms of the Last 2000 Years*, edited by P.D. Jones, R.S. Bradley, and J. Jouzel, pp. 43-66, Springer-Verlag, New York, 1996.

Welch, P.D., The use of fast Fourier transform for the estimation of power spectra: A method based on time averaging over short modified periodograms, *IEEE Trans. Audio Electroacous.*, *AU-15*, 70-73, 1967.

Wigley, T.M.L., K.R. Briffa, and P.D. Jones, On the average value of correlated time series with applications in dendroclimatology and hydrometeorology, *J. Clim. Appl. Meteorol.*, *23*, 201-213, 1984.

K.R. Briffa, I.C. Harris, P.D. Jones, and T.J. Osborn, Climatic Research Unit, University of East Anglia, Norwich NR4 7TJ, England. (k.briffa@uea.ac.uk; i.harris@uea.ac.uk; p.jones@ uea.ac.uk; t.osborn@uea.ac.uk)

F.H. Schweingruber, Swiss Federal Institute for Forest, Snow and Landscape Research, Zurcherstrasse 111, CH-8903 Birmensdorf, Switzerland. (fritz.schweingruber@wsl.ch)

S.G. Shiyatov, Institute of Plant and Animal Ecology, Ural Branch of the Russian Academy of Sciences, 8 Marta Street 202, Ekaterinburg 620144, Russia. (stepan@ipae.uran.ru)

E.A. Vaganov, Institute of Forest, Akagemgorodok, Krasnoyarsk 660036, Russia. (eavaganov@forest.akadem.ru)

(Received July 10, 2000; revised September 8, 2000; accepted September 13, 2000.)